Assessment of friction stir welds with nondestructive methods

Lévesque, Daniel; Dubourg, Laurent; Mandache, Catalin; Gougeon, Patrick; Cao, Xinjin; Jahazi, Mohammad

Publisher's version / la version de l'éditeur:
COM2008Winnipeg : Conference of Metallurgists, proceedings, 2008

ASSESSMENT OF FRICTION STIR WELDS WITH NONDESTRUCTIVE METHODS

*D. Lévesque[1], L. Dubourg[2], C. Mandache[2], P. Gougeon[1], X. Cao[2] and M. Jahazi[2]

[1]Industrial Materials Institute (IMI-NRC)
75 de Mortagne,
Boucherville, Quebec, Canada J4B 6Y4
*(*Corresponding author: daniel.levesque@cnrc-nrc.gc.ca)*

[2]Institute for Aerospace Research (IAR-NRC)
1200 Montreal Road,
Ottawa, Ontario, Canada K1A 0R6

ABSTRACT

Different nondestructive evaluation (NDE) methods are proposed for the detection of defects specific to friction stir welds (FSW). Ultrasonic immersion or laser-ultrasonics combined with the synthetic aperture focusing technique (SAFT) is investigated. Laser-ultrasonics uses lasers for the generation and detection of ultrasound and is therefore non-contact ultimately for weld assessment during welding. The pulsed eddy current (PEC) technique is also considered in this study as providing a good material penetrability. Analysis of the time-domain signal makes use of the lift-off point of intersection (LOI) feature as an indication of material condition. FSW lap and butt joints for aerospace applications and tailor welded blanks for automotive applications are examined, including the case of dissimilar metal welds. Very good performances are achieved with the two methods for lack of penetration in butt joints, the detection limit coinciding with the conditions of reduced mechanical properties. Also, discontinuities such as wormholes, hooking and voids are clearly detected using SAFT. The detection of kissing bonds seems to be possible in lap joints using high frequency laser-ultrasonics.

INTRODUCTION

During the last few years, FSW has been gaining acceptance and has found various applications in aerospace, automotive, railway and naval industries. In the aerospace industry, stronger and lighter friction stir welded joints are excellent candidates for replacing bonded and riveted joints in the manufacture of large fuselage and other components. Validation of the desired weld quality is done by both destructive and nondestructive testing. However, the nondestructive inspection of FSW is not yet clearly established, especially due to specific defects and their random orientation within the weld. Typical defects are lack of penetration, wormholes and kissing bonds (vertical) in butt joints, and hooking, wormholes and kissing bonds (horizontal) in lap joints. Kissing bonds originate from the remnants of trapped oxide layers resulting in inferior mechanical properties in the weld nugget [1]. They are known as the most challenging problem for inspection of FSW joints. This opens the way to novel nondestructive evaluation (NDE) procedures which have the potential to detect particular friction stir weld discontinuities. The use of NDE methods at the manufacturing stage could also provide good indications of the possible inspection challenges that may occur later on, while the friction stir welded component is in service.

The National Research Council Canada (NRC) has launched a series of initiatives regarding various aspects of FSW, starting from manufacture and its process control, to analysis of weld microstructure and residual stresses. The NDE aspect is of paramount importance when certification and industrialization of the FSW technique are considered. To date very limited results have been reported on non destructive detection of the defects described above [2-4]. Both ultrasonic-based methods and eddy current techniques have been found promising for this purpose; however, their actual performance for detecting defects, particularly for kissing bonds is still uncertain. Moreover, little data exists on the relationship between nondestructive testing information and the quality of the weld in terms of its mechanical performance.

In this paper, an ultrasonic technique combined with numerical focusing and processing is proposed. Data acquisition over a line across the weld at regular intervals is made using a conventional immersion technique or a laser-ultrasonic technique. The laser-ultrasonic method uses lasers for the generation and detection of ultrasound, and is therefore very broadband and non-contact, ultimately for weld assessment during welding. Numerical focusing is achieved with a Synthetic Aperture Focusing Technique (SAFT) algorithm. Another promising NDE method, pulsed eddy current (PEC) technique is considered in this study. Pulsed excitation provides a good material penetrability compared to conventional, sinusoidally excited eddy current testing. The pulse is equivalent to a multitude of simultaneous single frequency inspections. This method detects defects based on electrical conductivity changes and most sensitive signal features to specific weld discontinuities are investigated.

Various FSW lap and butt joints for aerospace applications and tailor welded blanks (TWB) for automotive applications are examined, including the case of dissimilar metal welds. Immersion and laser-ultrasonic results with SAFT as well as PEC results are presented with measurements on opposite and same sides relative to the welding tool. The testing with NDE methods, metallography analysis and validation by destructive mechanical testing are carried out. The detection limit for each technique and a comparison with joint mechanical performances are also discussed.

DESCRIPTION OF THE NDE METHODS

Ultrasonic Inspection with SAFT

One approach to detect the different types of flaws in FSW is illustrated in Figure 1. For use with SAFT, the generation and detection zones overlap at the surface of the part. An immersion technique with a piezoelectric transducer focused on the surface can be considered. A broadband focused transducer from Panametrics provided a frequency content up to 50 MHz. Alternatively, laser-ultrasonics can be considered for non-contact inspection [5, 6]. To achieve much higher frequencies, the generation of ultrasound was performed in the slight ablation regime with a 35 ps duration pulse of a Nd:YAG laser in its 3rd harmonic

with a spot size of about 50 μm. The detection uses a long pulse Nd:YAG laser in conjunction with a photorefractive interferometer for demodulation. Frequencies up to 220 MHz were successfully generated and detected in the weld region. Mechanical scanning along two axes was performed for data acquisition with a step size of 0.1 mm.

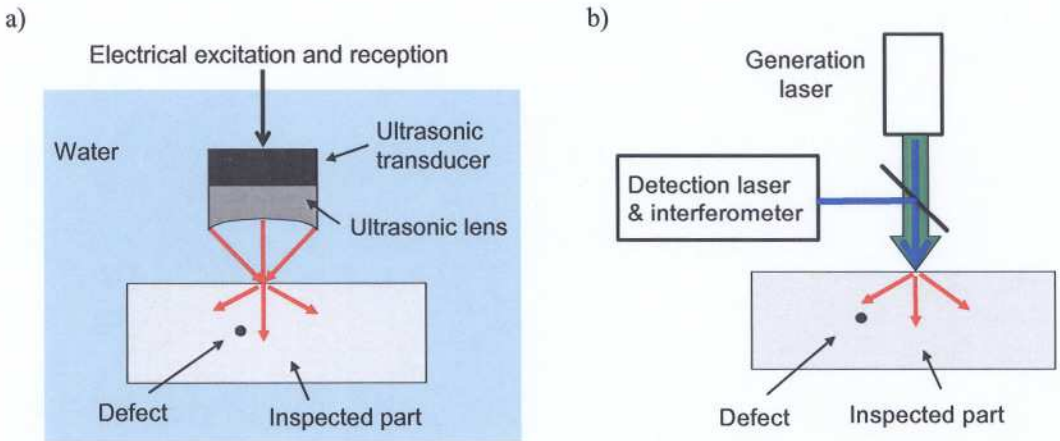

FIGURE 1 - Measurement setups that can be used for inspection of FSW with SAFT. a) Immersion technique and b) laser-ultrasonics

For the numerical focusing, a SAFT algorithm in the Fourier domain is used for time-efficient reconstruction [7, 8]. Processing the data with SAFT allows synchronization of the ultrasonic signals backscattered in different directions from each point in the weld region. The numerical focusing presents similarities with ultrasonic phased array system but makes it easier for detecting flaws at shallow depths such as those found in the joining of thin plates. Both immersion and laser-ultrasonic results with SAFT are presented in the following sections with measurements on opposite and same sides relative to the welding tool. The scans are performed after the removal by milling of any welding debris that could interfere with the recorded signal.

Pulsed Eddy Current Inspection

While ultrasonic techniques could not be used for layered structures due to the inability of the waves to penetrate through possible air gaps and conventional eddy current methods suffer due to low penetrability, pulsed eddy current inspection seems a viable alternative. This technique uses a pulse or square wave excitation and has the capability of deep penetration of conductive materials (up to few mm), due to its broadband frequency content. Recently, Smith successfully investigated the relationship between the electrical conductivity by PEC and the hardness of FSW coupons [9]. This work also showed promising results for monitoring other material properties and microstructure using the PEC method. The inspection and data analysis in this paper make use of the lift-off point of intersection (LOI) feature. This signal feature is based on the existence of a crossing point in the time-domain PEC response which is independent of lift-off. This feature has been successfully used for detection of cracks and corrosion in multi-layered structures. The use of the LOI is well documented in the specific literature [10, 11].

A R/D Tech transmit-receive sliding probe P11705 was used for these experiments, with the coils alignment along the weld direction, coils diameter of 6.5 mm and a centre-to-centre coil separation of 8 mm. The probe was voltage driven, with a square function of 10 V amplitude, and a pulse width of 500 μs. The output signal is band-pass filtered (100 Hz - 300 kHz) and amplified. The resolution was set to 0.5 mm on both scanning and indexing axes. Also with this method, the scans are performed from the welding side after the removal by milling of any welding debris that could interfere with the recorded signal.

RESULTS ON LAP JOINTS

All welds were produced on a MTS I-STIR FSW machine. The standard tool with a scrolled shoulder (19 mm diameter) and a pin (6.3 mm diameter pin) was used for all welds. The tool tilting angle was adjusted at 0.5°. Three lap joint samples using FSW for aerospace application, consisting of a 1.5 mm thick plate of AA7075-T6 on top of a 2.5 mm thick plate of AA2024-T3, were performed with different pin shapes (truncated pin, no-threaded cylindrical pin and threaded cylindrical pin) and welding parameters (welding speed, tool rotation speed, shoulder penetration) in order to create different defects.

Figure 2 shows an ultrasonic SAFT image of a cross-section (as B-scan) and corresponding metallography of a lap joint. The presence of hooking near the interface in both the advancing side and the retreating side is clearly visible. Results are shown for immersion on the weld side (tool side), but good images were also obtained from the opposite side with the hooking defect oriented downwards. SAFT reconstruction is found very useful for the identification of hooking defect by properly reducing the size of indications having a parabolic shape. The SAFT image also shows a void at this particular location along the weld.

a) b)

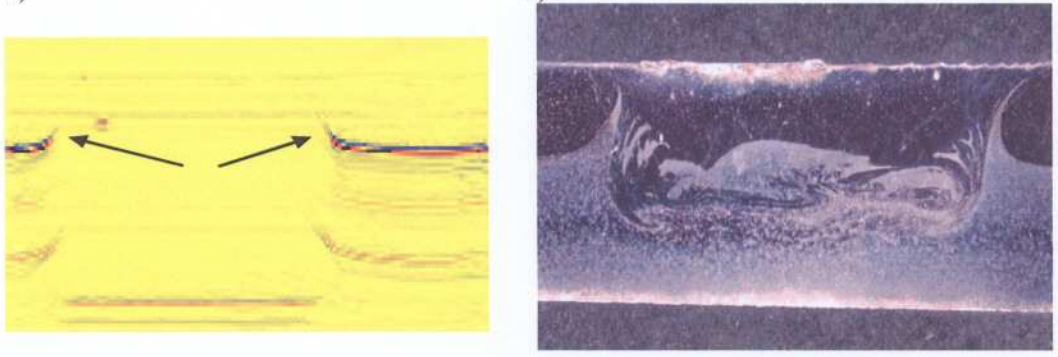

FIGURE 2 - Cross-section of a first lap joint with the presence of hooking. Welding parameters: truncated pin, welding speed of 500 mm/min, spindle speed of 800 RPM, shoulder penetration of 0.1 mm. a) SAFT image (B-scan) obtained by immersion on the weld side and b) corresponding metallography

a) b)

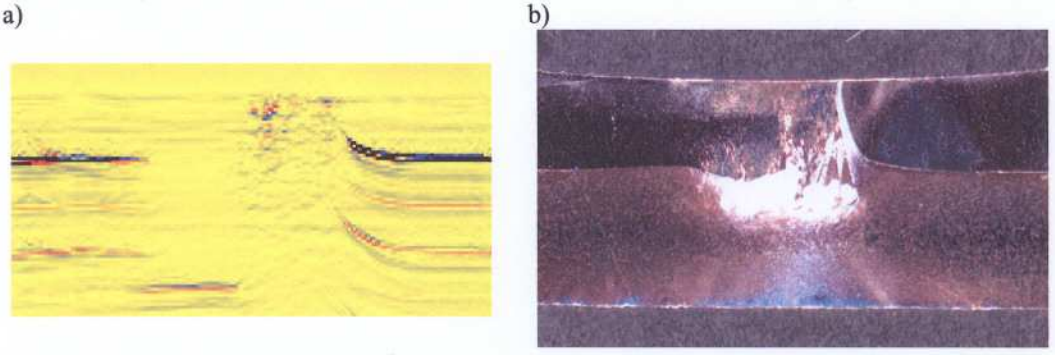

FIGURE 3 - Cross-section of a second lap joint with many defects. Welding parameters: no-threaded cylindrical pin, welding speed of 500 mm/min, spindle speed of 1000 RPM, shoulder penetration of 0.1 mm. a) SAFT image obtained by immersion on the weld side and b) corresponding metallography

A second lap joint is presented in Figure 3 with hooking in the advancing side, as well as indications of a wormhole above the interface. A wormhole occurs when the feed ratio is too high or too low, the feed ratio being the ratio between the welding speed and the tool rotation speed [12]. These results are for immersion on the weld side (tool side). Figure 4 shows SAFT images obtained from the opposite

side using immersion (frequencies up to 50 MHz) and laser-ultrasonic inspection (frequencies up to 220 MHz). The presence of hooking defect oriented downwards on one side as well as a similar wormhole, below the interface when viewed from the weld side, are observed with better resolution when using laser-ultrasonics. More importantly, a kissing bond present in the weld is detected by laser-ultrasonics as a slight reflection along the interface and above that from the weld surface. This capability was confirmed by the detection of another kissing bond defect in a similar sample.

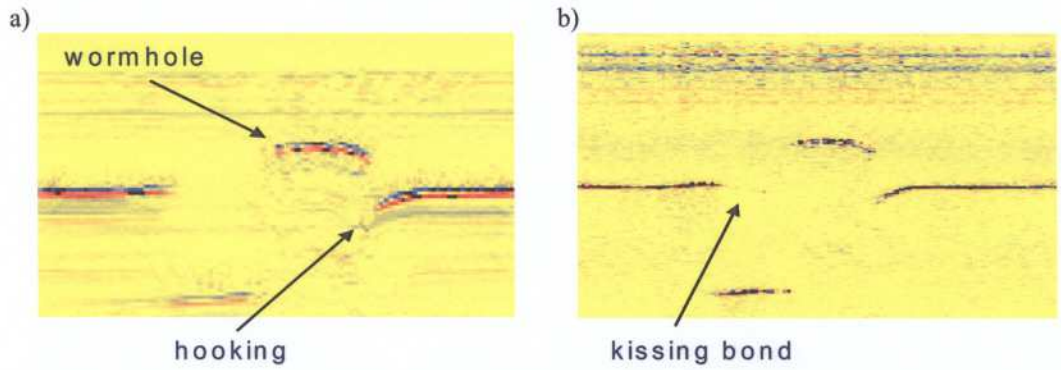

FIGURE 4 - Cross-section of the lap joint in Figure 4, with inspection from the far side of the tool. SAFT image using a) immersion and b) laser-ultrasonics

The first lap joint specimen was also inspected by PEC, with the goal of mapping the conductivity of the weld under the conditions of mixing two alloys of different conductivities, stirred at high temperature. The PEC scan was performed from the top side of the weld. First, a calibration curve was established based on the LOI point coordinates for seven Zetec conductivity standards: 9.32, 29.52, 31.82, 37.78, 48.44, 59.01, and 87.55 %IACS. Then, two different scans were performed, at two different applied lift-off values: 0.0 mm and 0.5 mm. For each individual point measurement in the scan, the LOI could be found as the intersection of the two signals, corresponding to the two lift-off values. Either the LOI time or the LOI amplitude on the conductivity calibration curve previously determined could be used for quantifying the conductivity. The LOI amplitude was chosen for interpreting the scan since it provided a higher rate of change with conductivity.

Figure 5 shows a contour map of the lap joint specimen in terms of electrical conductivity. For PEC inspection, the top layer has an electrical conductivity of 31.5 %IACS, while the second layer has a conductivity of 49.6 %IACS. It could be observed that in the area around the beginning of the weld, near the location of the pin plunge in the material, the conductivity ranges between 31 and 35 %IACS, which is higher than the conductivity of the top layer, but lower than the conductivity of the second layer. In the weld zone, the conductivity map indicates lower values than that of the top material, of about 25-26 %IACS. Away from the weld, in the transverse direction, the conductivity is closer to the one of the bulk top material, without indicating influences from the weld. The lower conductivity of the weld region may be related to the formation of finer grains in the weld center than in the parent material. Grain boundaries act as barriers in the movement of the free charges in the metal resulting in increased resistivity and lower conductivity. The lower conductivity may be also related to changes in the dislocation density. Indeed, dislocation density in the weld nugget may be lower than that in the base metal due to recrystallization. Although the conductivity is sampled at the surface, it contains partial through-thickness conductivity information, as a result of the PEC capability to penetrate few mm deep in the specimen. The conductivity map shown in the figure represents a weighted influence over the area of the pick-up coil and the volume under it, corresponding to the magnetic field diffusion and penetration in the metal.

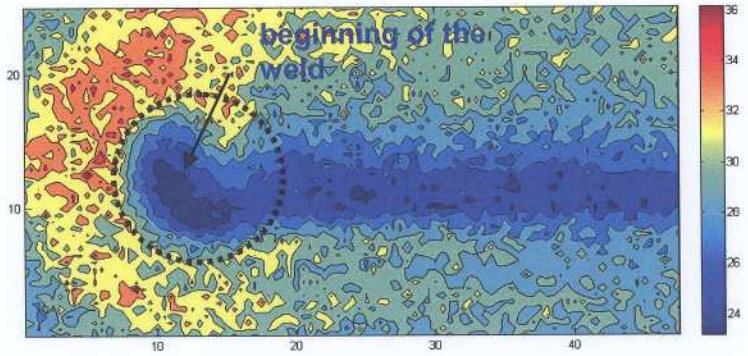

FIGURE 5 - Conductivity map determined based on LOI amplitude and conductivity calibration curve. The color bar on the right indicates the conductivity scale in %IACS

RESULTS ON BUTT JOINTS

Two sets of samples using FSW for aerospace application were welded in butt configuration. The first set was performed on 2-mm thick AA7075-T6 sheets with a conductivity of 31.5 %IACS with a tool composed of a concave shoulder (diameter of 10 mm) and a threaded cylindrical pin (pin diameter of 3 mm). The pin length was purposely made too short (1.2-mm long) in order to generate a lack of penetration (LOP). Figure 6 shows a SAFT image and the corresponding metallography of a cross-section of a butt joint with a constant LOP. Measurements were made by laser-ultrasonics on the weld side to detect the LOP on the opposite side. The LOP is well observed and appears as a lack of signal of the longitudinal (L) wave near the bottom surface. From metallography, the LOP shown has a width of about 10 μm and a depth of 0.6 mm, but the detection of a 0.3 mm deep LOP in a similar specimen was also observed. However, the quantitative estimation of the depth appears difficult, a situation similar to that found in a previous work for crack detection [13]. Also, the shear wave, usually generated in laser-ultrasonics, was too weak in this Al alloy and not practical for SAFT reconstruction.

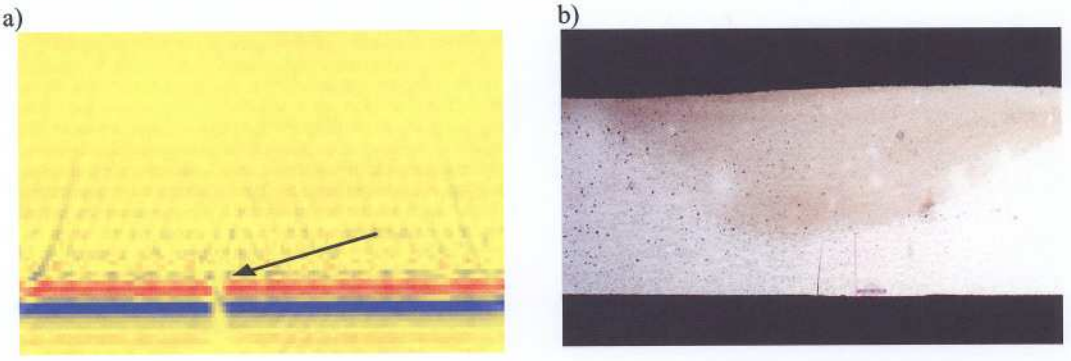

FIGURE 6 - Cross-section of a butt joint showing a lack of penetration in 2-mm thick AA7075-T6 butt weld. a) SAFT image and b) corresponding metallography

The same specimen was also PEC inspected. The LOI feature is identified before the actual scan, by manually changing the probe lift-off. Once the LOI cross-over point was found, the C-scans represent the voltage amplitude sampled in a small time gate of 2 μs, centered on the LOI. While the LOI feature eliminates possible lift-off variations, it detects the actual changes in the PEC signal response introduced by the weld, but it is not sufficient for observing the actual lack-of-penetration defect. This is due to both defect orientation and size. However, some simple image processing algorithms using background subtraction and Sobel filtering easily revealed the existence of the lack-of-penetration defect as shown in Figure 7. The Sobel operator calculates the image intensity gradient and is commonly used in image

processing, where it is employed to identify edges [14]. Consequently, the existence of an abrupt change in the PEC signal may be indicative of a discontinuity, as in this case of LOP defect.

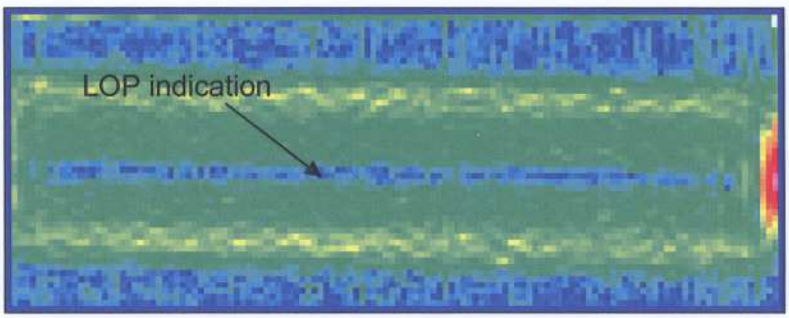

FIGURE 7 - C-scan image from PEC at LOI of the butt-joint sample, after applying edge identifier and background subtraction operators

Even though quantitative determination of depth is uncertain with both methods, a comparison of the limit of detectability with mechanical performance was investigated. For this purpose, a second set of butt welds was performed on 2.5-mm thick AA2024-O sheets with a conductivity of 49 %IACS with a tool composed of a scrolled shoulder (diameter of 19 mm) and a threaded cylindrical pin (pin diameter of 6.3 mm). For this experiment, the pin penetration was progressively increased from 1.2 mm to 2.5 mm during welding along the 355-mm in length joint. This operation introduced a variable weld depth and, consequently, a gradual LOP on the back-side of the weld. Metallographic examination at several locations along the weld revealed a LOP for a total penetration of the rotating tool (shoulder and pin) lower than 2.2 mm from the top surface. It is well known that, to produce a good weld, the pin does not have to touch the bottom surface of the plate because of the stirring action of the pin during FSW.

Laser-ultrasonic inspections of regions of dimensions 10 mm x 10 mm were performed along the weld at regular intervals. Figure 8 shows the SAFT images of the bottom surface at different locations, with the numbers giving the pin penetration at the center of each image, increasing only slightly from left to right. Indications of LOP along the weld are well observed for pin penetrations less than 2.2 mm, starting from a continuous line and finishing with an irregular trace. The irregular appearance of a LOP could imply that many cross-sectional views are required for evaluating the weld quality by metallography. Also, the mixed or alternate presence of LOP with vertical kissing bonds that are more difficult to detect is possible. As an evaluation of the weld integrity, bending tests were performed on different portions of the butt joint sample with variable pin length. Using optical microscopy, no failure was observed for pin penetration larger than 2.14 mm. This is in good agreement with the SAFT results as well as with those from metallography. Interestingly, this is one example supporting the idea that the limit of detectability with NDE may coincide with the conditions of reduced joint mechanical performances. Additional tests are in progress to confirm this observation.

With PEC measurement, inspection procedure and signal processing conditions similar to the ones mentioned above were used. In Figure 9a, the scan result using the LOI feature alone identifies the changes in the weld depth by a wider region as the pin depth is increased from left to right, but not the LOP defect. The weld is indicated by the changes in electrical conductivity associated with the extension of the heat-affected zone due to the welding tool shoulder contact with the plate. Figure 9b shows the C-scan image after applying the Sobel magnitude edge identifier filtering, allowing visualization of the LOP defect. It is believed that quantification in terms of defect depth would be possible by manufacturing reference blocks of know LOP depths.

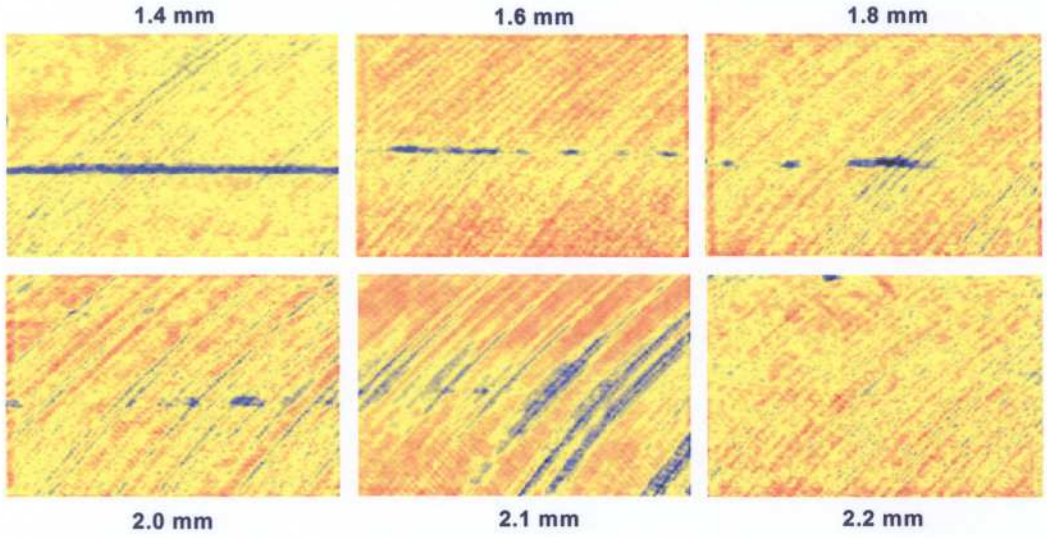

FIGURE 8 - SAFT images of the bottom surface for different pin penetrations as indicated along the weld

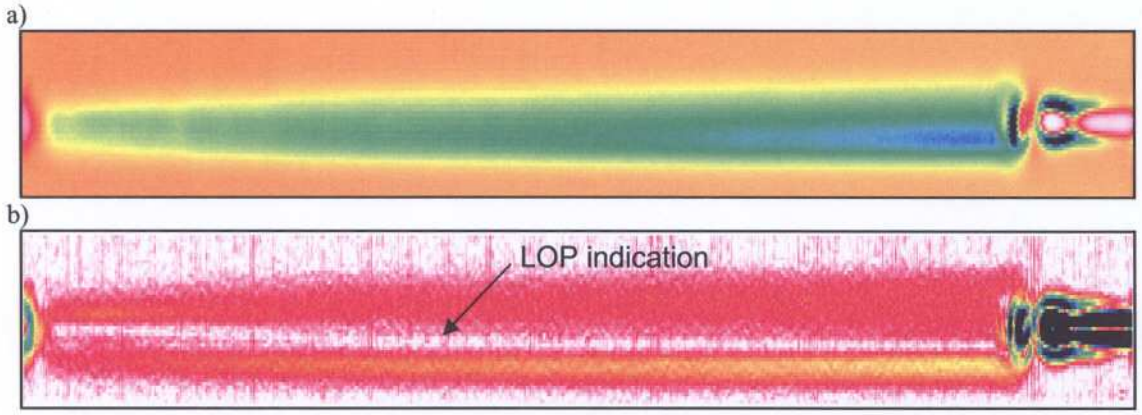

FIGURE 9 - C-scan image from PEC at LOI of the butt-joint sample with a variable pin depth a) before and b) after applying edge identifier and background subtraction operators

RESULTS ON TAILOR WELDED BLANKS

Tailor welded blanks (TWB) of aluminum are being produced by FSW to join different thicknesses for applications to automotive panels and structures while keeping high strength joints and reducing the vehicle weight.

A set of four TWB welds were produced on a MTS I-STIR FSW machine. The standard tool with a cup shoulder (10.9 mm diameter) and a pin (5.3 mm diameter) was used for all welds. The roll tool angle was adjusted at 3.5° and the pitch tool angle at 8.5°. The TWBs consisted of a 3.2 mm thick plate of Al-6061-T6 in contact with a 1.9 mm thick plate of the same alloy. The FSW were performed with different pin shapes and lengths (cylindrical threaded pin with various pin lengths and diameters) and welding parameters (welding speed, tool rotation speed, shoulder penetration) in order to create different defects. Figure 13 shows one metallography of a TWB specimen where oxide flaws, root flaws and wormholes of diameters between 50 and 400 μm are observed.

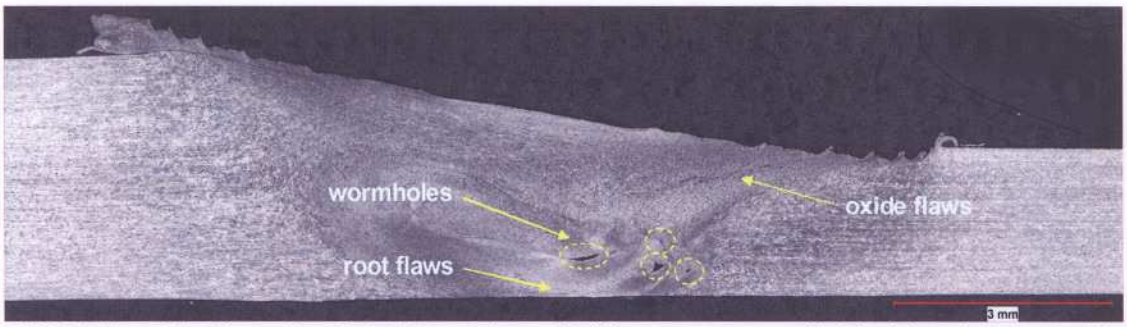

FIGURE 10 - Metallography of a TWB specimen. Welding parameters: cylindrical threaded pin, welding speed of 1200 mm/min, spindle speed of 1500 RPM, shoulder penetration of 0 mm

Figure 11 shows ultrasonic SAFT images of cross-sections at two locations. Results are shown for immersion and inspection on the weld side (tool side), with the sample inclined to make the surface of inspection horizontal. Three or four wormholes are well observed along the weld axis in both cross-sections. There is also an indication of a root flaw on the bottom surface in Figure 11a. In some locations along the weld path axis such as in Figure 11b, there is a strong indication above which (about 1 mm) that appears to be more a void rather than the oxide flaws observed in the metallography.

a) b)

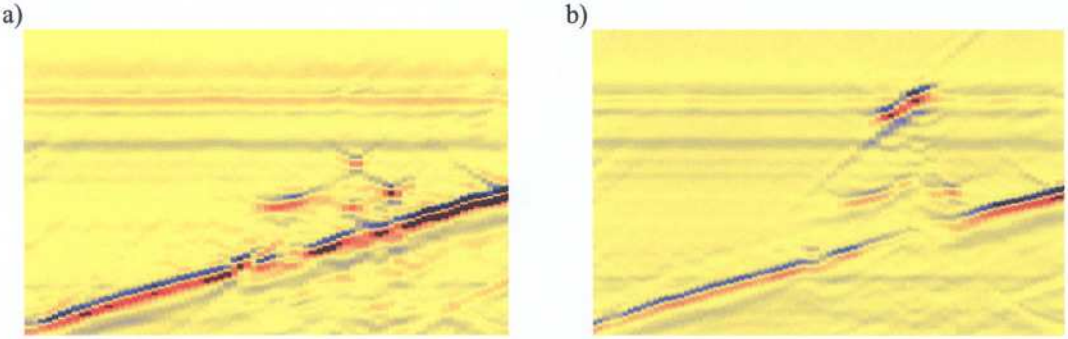

FIGURE 11 - a) SAFT image of a cross-section of a TWB specimen with the presence of wormholes and b) another cross-section also presenting a defect 1 mm above

a) b)

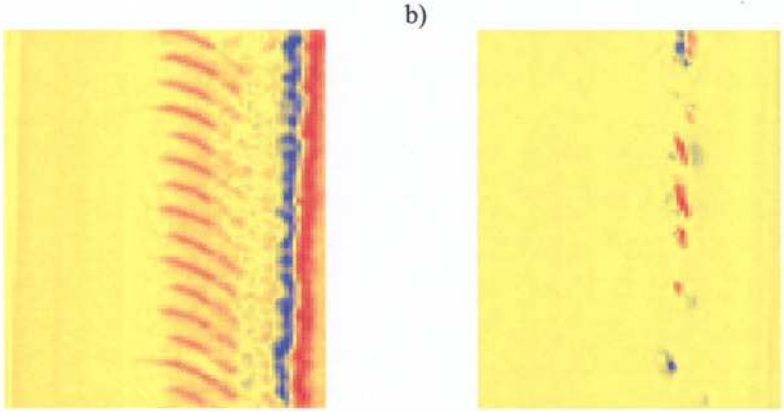

FIGURE 12 - SAFT image of sub-surface planes of the TWB specimen a) at the level of the wormholes in Figure 11a and b) 1.0 mm above

Figure 12a shows a SAFT image of a subsurface plane at the level of the wormholes. Figure 12b shows the presence of the voids 1 mm above as discussed and appearing in an irregular manner. Again, this indicates the need of many cross-sectional views for evaluating the weld quality by metallography as compared to ultrasonic SAFT or PEC inspection. Also, the combined or alternate presence of voids with oxide flaws is possible.

RESULTS ON DISSIMILAR METAL WELDS

Dissimilar metal welds of aluminum and magnesium by FSW are being considered for automotive and aerospace applications. Complex vortex flows are produced during the FSW process that may create intercalated lamellar structures with the possible formation of intermetallic compounds such as $Al_{12}Mg_{17}$, causing variable hardness and degradation in mechanical properties, especially ductility. Three welded samples consisting of 5-mm thick Mg AZ31 and AA 2024 sheets in the butt configuration were prepared with welding speeds of 0.75, 9.0 and 15.0 mm/s.

Measurements were performed using the immersion technique on the weld side (tool side) with a modified version of SAFT to take into account the difference of ultrasonic velocity in the joint between that of Al (6.4 mm/μs) and Mg (5.8 mm/μs). Figure 13 shows an ultrasonic B-scan or cross-section of a dissimilar metal weld before SAFT processing where the bottom echo (between cursors) appears at different levels. An example of the fit of the velocity transition (normalized, ranging from 0 to 1) between Al and Mg using the bottom echo is also shown. Embedded in the SAFT processing, such fitting through all B-scans allows getting an effective velocity for the propagation between each scattered point and measurement point combination.

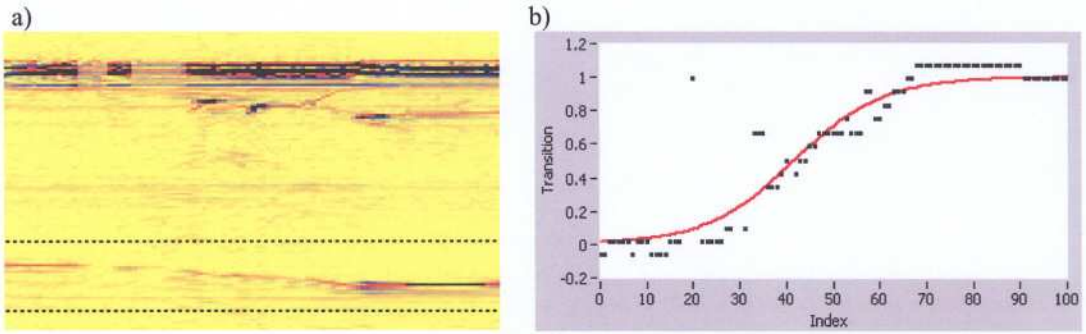

FIGURE 13 - a) B-scan or cross-section of a dissimilar metal weld before SAFT and b) fit of the velocity transition between Al (left) and Mg (right) using the bottom echo

Figure 14 shows C-scan images after modified SAFT processing near the mid-plane for the three specimens, the weld path axis being vertical. The weld produced with the lowest speed has a wide wavy pattern probably indicating a strong stirring and mixing of the two materials. The case of the highest welding speed also shows an apparent but more regular boundary between the two parent materials. While preliminary, these distinguishable results seem to demonstrate the potential of using nondestructive methods to evaluate dissimilar friction stir welds. Also, the relation between these indications and the presence of intermetallic compounds remains to be investigated.

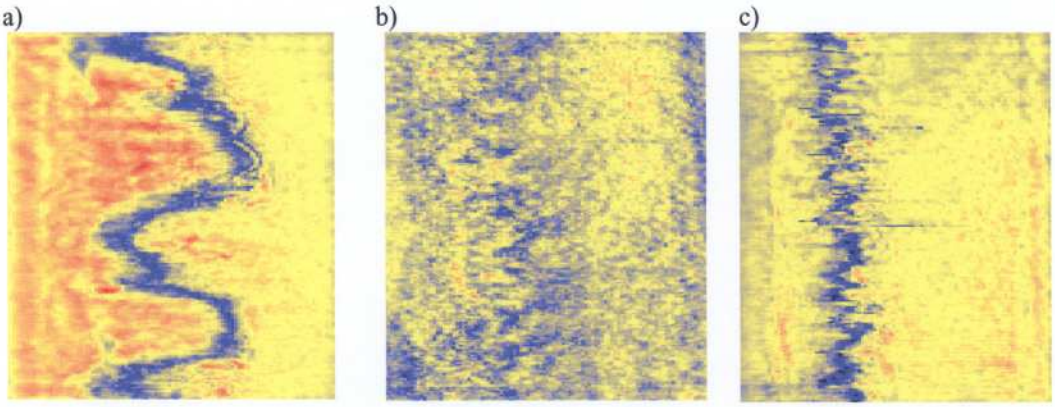

FIGURE 14 - SAFT image of sub-surface planes in the 3 butt joint specimens performed with a welding speed of a) 0.75 mm/s, b) 9.0 mm/s and c) 15.0 mm/s

CONCLUSION

Friction stir welding is increasingly gaining acceptance in different branches of transport industry. The NDE community is investigating the applicability of various techniques and their capability to detect specific discontinuities in friction stir welded components, both at the manufacture and in-service stages.

The applicability of the SAFT technique for the evaluation of friction stir welds using immersion ultrasonic technique and laser-ultrasonics is demonstrated. Measurements on the same or opposite side of the welding tool for both lap and butt joints of 1 to 2.5-mm thick aluminum sheets were carried out. Discontinuities such as wormholes, hooking, lack of penetration and voids are clearly detected in the lap, butt and TWB configurations. Moreover, the detection of kissing bonds seems possible in lap joints using high frequency laser-ultrasonics. Lack of penetration defects in butt joints were shown to be irregular, which means that many cross-sectional views may be required when using metallography. Also, the limit of detectability was found to coincide with the conditions of reduced mechanical properties. The approach could allow fast scanning for weld integrity assessment along the tool path.

The present study also showed that PEC technique has the ability to simultaneously detect flaws, such as lack of penetration and voids, and to sense conductivity changes that could be related to weld hardness and residual stresses in FSW joints. Reliable detection of critical flaws in FSW components will probably have to combine two or more NDE inspection techniques, capable to complement one another. Data fusion algorithms for the results obtained with different NDE methods are currently considered.

ACKNOWLEDGEMENTS

The authors would like to thank Lotfi Toubal for ultrasonic immersion measurements, André Gagnon and Marc Gallant for the metallographic examination of the specimens, as well as François Nadeau and Maxime Guérin for carrying out the FSW trials. This work was funded in the framework of National Research Council Canada horizontal programs through an inter-institute collaboration between the Industrial Materials Institute and the Institute for Aerospace Research.

REFERENCES

1. Y.S. Sato, H. Takauchi, S.H.C. Park and H. Kokawa, "Characteristics of the kissing-bond in friction stir welded Al alloy 1050", Mat. Sci. Eng., Vol. A 405, 2005, 333-338.

2. D. Kleiner and C.R. Bird, "Signal processing for quality assurance in friction stir welds", Insight, Vol. 46, 2004, 85-87.

3. A. Lamarre, O. Dupuis, M. Moles, "Complete inspection of friction stir welds in aluminum using ultrasonic and eddy current arrays", Canadian Institute for NDE Journal, Vol. 27, No. 4, 2006, 14-21.

4. S. Iwaki, T. Okada, N. Eguchi, S. Tanaka, K. Namba and N. Oiwa, "Imperfections in friction stir welded zones and their precision non-destructive testing. Studies on characteristics of friction stir welded joints in structural thin aluminium alloys", Welding Intern., Vol. 20, 2006, 197-205.

5. C.B. Scruby and L.E. Drain, "Laser-Ultrasonics: Techniques and applications", Adam Hilger, Bristol, UK, 1990.

6. J.-P. Monchalin, "Laser-ultrasonics: from the laboratory to industry", Review of Progress in Quantitative Nondestructive evaluation Vol. 23A, ed. by D.O. Thompson and D.E. Chimenti, AIP Conf. Proc., New York, 2004, 3-31.

7. D. Lévesque, A. Blouin, C. Néron and J.-P. Monchalin, "Performance of laser-ultrasonic F-SAFT imaging", Ultrasonics, Vol. 40, 2002, 1057-1063.

8. B. Campagne, D. Lévesque, A. Blouin, B. Gauthier, M. Dufour, J.-P. Monchalin, "Laser-ultrasonic inspection of steel slabs using SAFT processing", Review of Progress in Quantitative Nondestructive Evaluation Vol. 21A, ed. by D.O. Thompson and D.E. Chimenti, AIP Conf. Proc., New York, 2002, 340-347.

9. R.A. Smith, "The potential for friction stir weld inspection using transient eddy currents", Insight – Non-destructive Testing and Condition Monitoring, Vol. 47, No. 3, 2005, 133-143.

10. J.R.S. Giguère, B.A. Lepine, J.M.S. Dubois, "Pulsed eddy current (PEC) characterization of material loss in multi-layered structures", Canadian Aeronautics and Space Journal, Vol. 46, No. 4, 2000, 206-208.

11. J.R.S. Giguère, B.A. Lepine, J.M.S. Dubois, "Detection of cracks beneath rivets via pulsed eddy current technique", Review of Progress in Quantitative Nondestructive Evaluation Vol. 21, ed. by D.O. Thompson and D.E. Chimenti, AIP Conf. Proc., New York, 2001, 1968-1975.

12. L. Dubourg, M. Jahazi, F.O. Gagnon, F. Nadeau, and L. St-Georges, "Process window optimization for FSW of thin and thick sheet Al alloys using statistical methods", Proc. of the 6th Intern. FSW Symposium, St-Sauveur (Qc), Canada, 2006.

13. D. Lévesque, M. Ochiai, A. Blouin, R. Talbot, A. Fukumoto and J.-P. Monchalin, "Laser-ultrasonic inspection of surface-breaking cracks in metals using SAFT processing", 2002 IEEE Intern. Ultras. Symp. Proc., New York, 2002, 732-735.

14. R. Kletter and P. Zamperoni, "Handbook of Image Processing Operators", John Wiley & Sons Ltd, Chichester, England, 1996.